BEYOND STANDARD MODEL PHYSICS AT THE LARGE HADRON COLLIDER AT CERN*

R. Alemany-Fernandez

Laboratório de Instrumentação e Física Experimental de Partículas
Av. Elias Garcia 14–1, 1000-149 Lisboã, Portugal

(Received November 15, 2006)

This conference report presents a compilation of some of the latest results on prospects for Extra Dimensions and Extra Gauge Bosons Models with two general purpose detectors of the Large Hadron Collider (LHC) at the European Laboratory for Particle Physics (CERN): A Toroidal LHC ApparatuS (ATLAS) and the Compact Muon Solenoid (CMS). The results presented here correspond, in most of the cases, to full simulation and full reconstruction of the hadron interactions at 14 TeV center of mass energy at low and(or) high luminosity. In general, theoretical and systematic uncertainties are considered in the final results.

PACS numbers: 12.90.+b, 14.80.–j

1. Introduction

Theoretical arguments predict the existence of physics Beyond the Standard Model (BSM). This is one of the reasons why the Large Hadron Collider (LHC) and its detectors are being built at the European Laboratory for Particle Physics (CERN). In this conference report, the most recent results, from the experimental (simulation) point of view, on Extra Dimensions and Extra Gauge Bosons searches will be reviewed. In particular, the A Toroidal LHC ApparatuS (ATLAS) and the Compact Muon Solenoid (CMS) Collaborations analyses will be considered here. The last section of this chapter will be devoted to an extremely important subject: once a signature is discovered in the detector, what is the theoretical model that better fits the experimental data? This issue gets raised because many BSM scenarios (including Supersymmetry) predict the same kind of topologies (however the discrimination between Supersymmetry and other BSM models will not be addressed here). This paper is organized as follows: Section 2 is devoted to

* Presented at the "Physics at LHC" Conference, Kraków, Poland, July 3–8, 2006.

Extra Dimensional Models; Section 3 to Extra Heavy Bosons theories; Section 4 explains how to distinguish different BSM signatures; finally Section 5 contains the Conclusions.

2. Extra dimensional models

2.1. Introduction

The main motivation for the development of theories beyond the Standard Model (SM) is the hierarchy problem, *i.e.*, why the gravity energy scale (or Planck Mass, $M_{\rm Pl}$) and the electroweak energy scale ($M_{\rm EW}$) are so different: $\sim 10^{19}$ GeV compared to $\sim 10^3$ GeV, respectively. Several possibilities have been suggested to solve this "naturality" problem: perturbative solutions like Supersymmetry, and non-perturbative solutions like Compositeness and Technicolor. Alternatively, one can exploit the geometry of space-time via Extra Dimensional Theories. In this section the experimental prospects for the following four Extra Dimensional models will be reviewed: Arkani–Dimopoulos–Dvali (ADD) Model [1], Randall-Sundrum (RS) or warped extra dimensions [2], TeV^{-1} size extra dimensions [3] and Universal Extra Dimensions (UED) [4].

2.2. The ADD model

There are two ways of producing Kaluza–Klein (KK) gravitons ($G^{\rm KK}$) in ADD models: via direct graviton production and via virtual exchange.

Direct graviton production:
ATLAS results for $pp \rightarrow$ jet $+ G^{\rm KK}$ [5]: the topology consists of a jet with high transverse energy ($E_{\rm T} > 500$ GeV), and a high missing transverse energy ($E_{\rm T}^{\rm miss} > 500$ GeV) from the undetected gravitons. The analysis also vetoes the leptons via isolation and identification criteria. The irreducible SM background consists of jet $+ Z \rightarrow$ jet $\nu\nu$ and jet $+ W \rightarrow$ jet $l\ \nu$. The analysis was based on ATLAS fast simulation and reconstruction programs. Fig. 1 (left) shows the $E_{\rm T}^{\rm miss}$ for the different signals and backgrounds for 100 fb^{-1} of integrated luminosity and 14 TeV of center of mass energy ($\sqrt{s}$). For $S/\sqrt{B} > 5$ (S and B are the number of signal and background events, respectively, that pass the selection criteria), with $S > 100$ and $p_{\rm T}^{\rm jet} > 1$ TeV the following discovering limits are achieved: $M_{{\rm Pl}(4+\delta)}$ (M_D in the plot) = 7.7 : 6.2 : 5.2 for $\delta = 2 : 3 : 4$, respectively. δ is the number of extra dimensions compactified in a radius (R). $M_{{\rm Pl}(4+\delta)}$, the Planck mass in the $4+\delta$ dimensions, is the compactification scale *i.e.* a fundamental scale above which new physics enters and modifies the results of the theory.

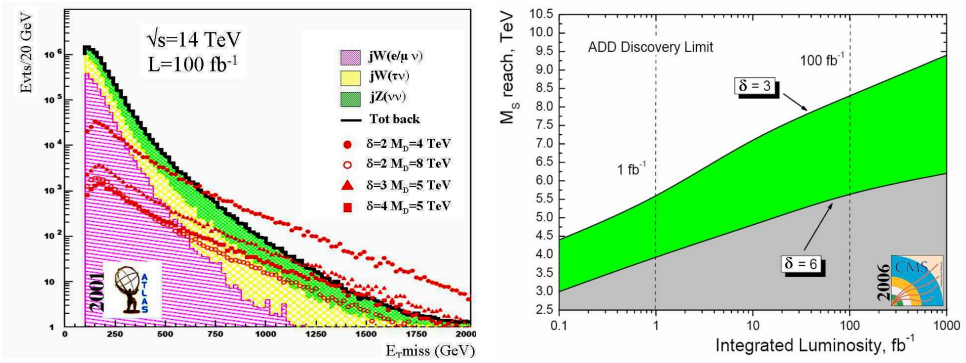


Fig. 1. Left: $E_{\mathrm{T}}^{\mathrm{miss}}$ for different ADD signals (different values of the parameter space) with jet and missing transverse energy in the final state and the corresponding irreducible backgrounds [5]. Right: ADD discovery limit of the compactification scale as a function of the integrated luminosity for graviton virtual production with 2 muons in the final state and for different values of the number of extra dimensions (δ) [7, 9].

CMS results for $pp \to \gamma + G^{\mathrm{KK}}$ [6, 7]: Another interesting signal at LHC is the production of a G^{KK} in association with a photon. Although the rates are much lower than in the jet case, and the region $(\delta, M_{\mathrm{Pl}(4+\delta)})$ which can be probed is much more limited, this signature could be used as a confirmation after the discovery in the jet channel. This topology will not be detectable in the low p_{T} region because the cross-section of the background, in particular the irreducible one, is too large. Therefore, a minimum $p_{\mathrm{T}} > 400$ GeV is consistently requested. The topology consists of a high E_{T} photon, produced in the central pseudo-rapidity region and back-to-back with respect to the missing transverse energy from the undetected gravitons. The irreducible SM background is $Z\gamma \to \nu\nu\gamma$. Other backgrounds also considered in this analysis are: $W \to e(\mu\tau)\nu$, $W\gamma \to e\nu\gamma$, γ+jets, Quantum Chromodynamic (QCD) background, di-γ, Z^0+jets. The estimated rates for cosmic muons (the biggest background in CDF detector at the Tevatron Collider in Fermilab) and beam halo muons for a $p_{\mathrm{T}} > 400$ GeV are 11 Hz and 1 Hz, respectively. Those backgrounds have not been considered in the CMS analysis yet. The results given in Table I correspond to CMS full simulation and reconstruction programs, with the significance calculated according to the expression [8]:

$$\mathcal{S} = 2(\sqrt{(S+B)} - \sqrt{B}) > 5\,. \tag{2.1}$$

As indicated in the table, the 5σ discovery reach of $M_{\mathrm{Pl}(4+\delta)} > 3.5$ TeV is not possible when including theoretical uncertainties.

TABLE I

Integrated luminosity needed in CMS for a 5σ significance discovery of the different parameter space values of the direct production of gravitons in the γ and missing energy final state [6].

$M_{\mathrm{Pl}(4+\delta)}/\delta$	2	3	4	5	6
1.0 TeV	0.21 fb^{-1}	0.16 fb^{-1}	0.14 fb^{-1}	0.15 fb^{-1}	0.15 fb^{-1}
1.5 TeV	0.83 fb^{-1}	0.59 fb^{-1}	0.56 fb^{-1}	0.61 fb^{-1}	0.59 fb^{-1}
2.0 TeV	2.8 fb^{-1}	2.1 fb^{-1}	1.9 fb^{-1}	2.1 fb^{-1}	2.3 fb^{-1}
2.5 TeV	9.9 fb^{-1}	8.2 fb^{-1}	8.7 fb^{-1}	9.4 fb^{-1}	10.9 fb^{-1}
3.0 TeV	47.8 fb^{-1}	46.4 fb^{-1}	64.4 fb^{-1}	100.8 fb^{-1}	261.2 fb^{-1}
3.5 TeV	5σ discovery not possible when including theoretical systematic uncertainties				

Virtual production of gravitons:
CMS results for $pp \to G^{\mathrm{KK}} \to \mu\mu$ [7,9]: the topology consists of two opposite sign muons with an invariant mass above 1 TeV. The cross-section is the sum of the SM contribution, the extra dimensional contribution and an interference term that is a function of $M_{\mathrm{Pl}(4+\delta)}$, δ and $\sqrt{s}$. The irreducible background is the Drell–Yan production of two muons. Other backgrounds also considered are ZZ, WZ, WW and tt, but they are successfully suppressed after the selection cuts. The signal and background were fully simulated and reconstructed. The following systematic uncertainties were taken into consideration: theoretical uncertainties, muon and tracker misalignment and trigger uncertainties. Fig. 1 (right) shows the $M_{\mathrm{Pl}(4+\delta)}$ (M_S in the plot) 5σ significance discovery reach, with $\mathcal{S}$ computed according to Eq. (2.1) for different values of δ.

2.3. The RS model

CMS results for $pp \to G_1^{\mathrm{KK}} \to \mu\mu, ee, \tau\tau$ [7,10–12]: at the LHC the RS $\mathrm{G}_1^{\mathrm{KK}}$ (the first KK excitation of the graviton) would be seen as difermion or diboson resonances, since the coupling of each KK mode is only TeV suppressed. The two model parameters are: c (the ratio of k, a scale of the order of the Planck scale, and M_{Pl}) and Λ_π (the scale of physical processes in the TeV brane). Fig. 2 shows the G_1^{KK} mass reach for dielectrons, diphotons and dimuons final states for different values of c and integrated luminosity. The region of interest is the one to the left of the curve $\Lambda_\pi < 10$ TeV (which is theoretically preferred [13]) and up to $c = 0.1$ because $c > 0.1$ is disfavoured on theoretical grounds as the bulk curvature becomes too large (larger than

the 5-dim Planck scale). The 5σ significance discovery areas are the regions to the left of the straight lines. The sensitivity to G_1^{KK} mass is calculated using the likelihood estimator [14] based on event counting suited for small event samples:

$$\mathcal{S} = \sqrt{(2[(S+B)\log(1+S/B) - S])} > 5\,. \tag{2.2}$$

The CMS analysis is based on full simulation and reconstruction, and includes the study of theoretical and experimental systematic uncertainties. As an example, Fig. 2 at the bottom shows the one sigma theoretical and experimental systematic uncertainties influence on the discovery limit. The misalignment scenario taken into account in the result corresponds to the first period of detector alignment obtained with ~ 1 fb^{-1} of data. During this period the muon reconstruction efficiency will be unaffected, while the momentum resolution will be reduced from 1–2% to 4–5%.

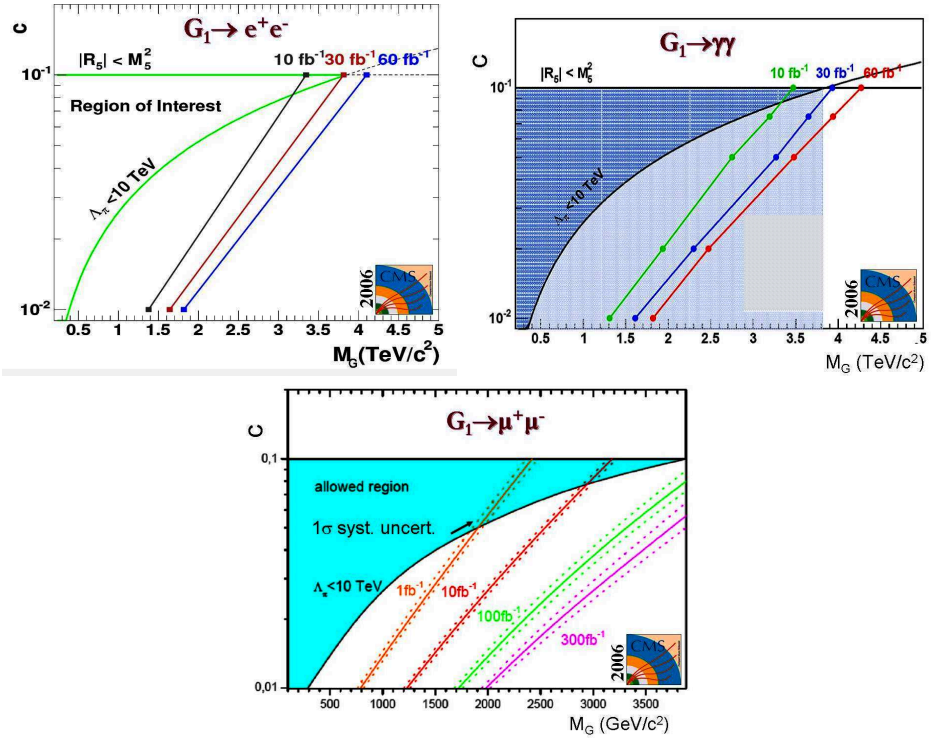


Fig. 2. G_1^{KK} mass reach for dielectrons, diphotons and dimuons final states, respectively, for different values of c and integrated luminosity. The 5σ significance discovery is the region to the left of the colored lines. The dimuon plot also shows the 1σ theoretical and experimental uncertainty on the integrated luminosity needed to reach the 5σ significance [7, 10–12].

2.4. The TeV^{-1} model

CMS results for $pp \to Z_1^{\mathrm{KK}}/\gamma_1^{\mathrm{KK}} \to ee$ [7,10]: the topology of this signature consists of two high p_{T} and isolated electrons produced from the decay of the first KK excitation of the Z or the γ. The electromagnetic energy associated to the electron candidate is corrected, among other things, for the energy leak in the hadronic calorimeter and for the Electromagnetic Calorimeter electronics saturation (because of the limited dynamic range of the Multi-Gain-Pre-Amplifier). The saturation takes place for energies above 1.7 TeV in the barrel and 3 TeV in the end-caps. The irreducible background is the Drell–Yan production of a pair of electrons. The signal and background are fully simulated and reconstructed with pile-up at low luminosity ($\sim 10^{33}$ cm^{-2}s^{-1}). Theoretical systematic uncertainties were also studied in detail. The discovery potential of the compactification scale (R^{-1}) is determined using Eq. (2.2). The results are shown in Fig. 3 (left). As can be seen, with an integrated luminosity of ~ 80 fb^{-1}, CMS will be able to detect a peak in the $e+e-$ invariant mass distribution if $R^{-1} < 6$ TeV.

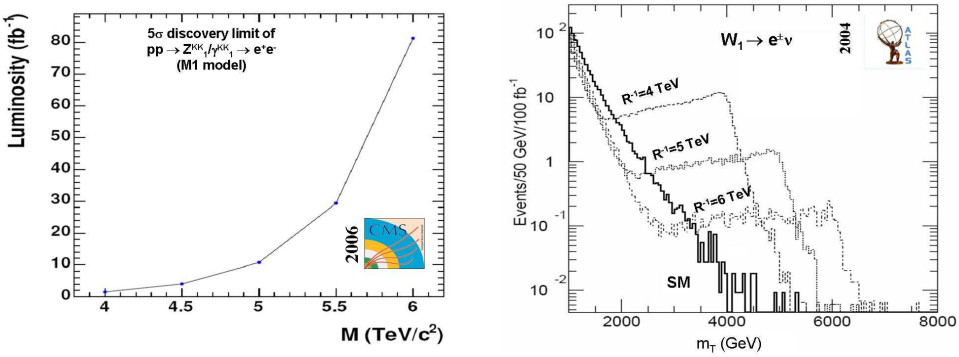


Fig. 3. Left: Five sigma discovery limit of the $Z_1^{\mathrm{KK}}/\gamma_1^{\mathrm{KK}}$ in the M1 TeV^{-1} Extra Dimensional model. The x-axis is the compactification scale and the y-axis is the integrated luminosity needed to reach a 5σ discovery [7,10]. Right: Invariant transverse mass distribution of $e\nu$, for the M1 model, for different values of the compactification scale (R^{-1}) [16]. The histograms are normalized to 100 fb^{-1}.

ATLAS results for $pp \to Z_1^{\mathrm{KK}}/\gamma_1^{\mathrm{KK}} \to ll$ $(l = e, \mu)$ [15]: ATLAS also performed a detailed study of the leptonic signatures from the production of $Z_1^{\mathrm{KK}}/\gamma_1^{\mathrm{KK}}$. The production and decay of the first excitations were fully simulated and the resulting particles were passed through a parameterized simulation of the ATLAS detector. The 5 sigma significance expression used to compute the results is the following:

$$\mathcal{S} = \frac{S-B}{\sqrt{B}} > 5 \quad \text{with} \quad S > 10\,. \tag{2.3}$$

The results show that with an integrated luminosity of 100 fb^{-1}, ATLAS will be able to detect a peak in the lepton–lepton invariant mass if $R^{-1} < 5.8$ TeV.

ATLAS results for $pp \to W_1^{\rm KK} \to \nu l$ [16]: The selection cuts to search for the decay of the first KK excitation of the W into νl consist of requiring one high $p_{\rm T}$ and isolated lepton (> 200 GeV) uniquely identified as an electron or muon. The events are also characterized by a high transverse momentum imbalance. The invariant mass of the pair (l, ν) should be larger than 1 TeV. A jet veto algorithm is also applied. The irreducible background is the SM production of $W \to \nu\, l$; other backgrounds also considered in the analysis but successfully suppressed were tt, WW, ZZ and WZ. The 5σ significance expression used to compute the discovery limit is the one given in Eq. (2.3) with at least 10 events summed over the two lepton flavors. Fig. 3 (right) shows the invariant transverse mass distribution of eν, for the M1 model [16], for different values of R^{-1}. The histograms are normalized to 100 fb^{-1}. It is found that with an integrated luminosity of 100 fb^{-1} the ATLAS detector will be able to detect a peak in the lepton-neutrino invariant transverse mass if $R^{-1} < 6$ TeV.

ATLAS results for $pp \to g_1^{\rm KK} \to b\overline{b}, t\overline{t}$ [17]: The presence of gluon excitations ($g_1^{\rm KK}$) is detected by analyzing deviations in the dijet cross-section. An alternative proposal by ATLAS is detecting $\rm g_1^{KK}$ by analyzing its decays to heavy quarks. The two b's final state topology is selected requesting two b-tagged jets with $p_{\rm T}^b$ cut which is a function of the $m(g_1^{\rm KK})$. In the case of the $g_1^{\rm KK}$ decaying into two tops, one top is forced to follow a leptonic decay. Therefore the selection criteria request a lepton with $p_{\rm T}^l > 25$ GeV, $E_{\rm T}^{\rm miss} > 25$ GeV, and two b-tagged jets (from the decay of the second top) with a given angular separation and a $p_{\rm T}^b$ cut which is a function of the $m(g_1^{\rm KK})$. The SM backgrounds taken into account were $b\overline{b}$, $t\overline{t}$, 2 jets and W + jets. The fast simulation and reconstruction programs of ATLAS were used to perform the analysis. The best discovery potential is achieved with the $t\overline{t}$ channel and corresponds to $R^{-1} = 3.3$ TeV for 300 fb^{-1} of accumulated data. Although this limit cannot compete with the dijet channel, the decay into two tops could be used to confirm the presence of a $g_1^{\rm KK}$ in case that an excess of events is observed in the dijet channel.

2.5. Universal extra dimensions

CMS results for $pp \to g_1^{\rm KK} g_1^{\rm KK}/Q_1^{\rm KK} Q_1^{\rm KK}/g_1^{\rm KK} Q_1^{\rm KK} \to 4l + m$ jets $+ 2\gamma_1^{\rm KK}$ [18]: The final state consists of four low $p_{\rm T}$ isolated leptons (two pairs of opposite sign same flavor leptons), a m number of jets and missing transverse energy from the two undetected $\gamma_1^{\rm KK}$. To improve the background rejection over the sig-

nal b-tagging and Z-tagging vetoes are applied. The irreducible backgrounds are $tt + m$ jets, $4b$, ZZ and Zbb. A study at the parton level indicated that other backgrounds, such as $ttbb$, Zcc, $Zcc + m$ jets and WWZ, either have negligible cross-sections or can be suppressed by basic kinematical cuts. The discovery sensitivity for different values of R^{-1} and different luminosities is shown in Fig. 4 (left).

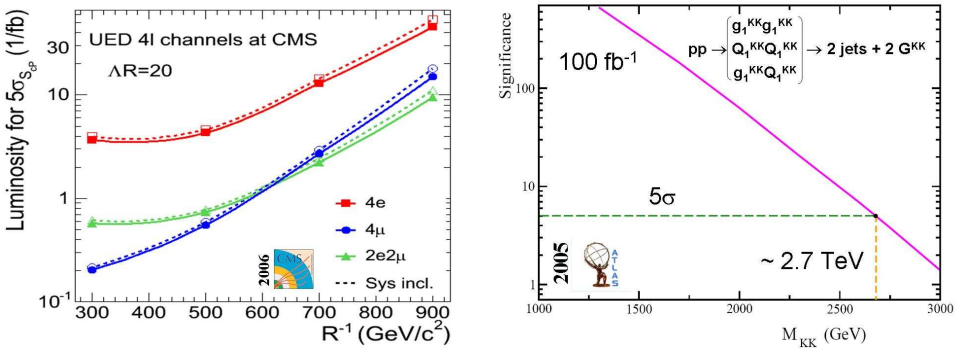


Fig. 4. Left: Required luminosity for a 5σ discovery in CMS of UED signals in the 4 leptons channel [18]. The systematic uncertainty corresponds to the level of 10–30 fb^{-1}. Additional systematic uncertainties expected in the initial phase (< 1 fb^{-1}) are not included. Right: Variation of the significance of the signal from fat brane scenarios as a function of the mass of the first KK excitation state for 100 fb^{-1} [19].

ATLAS results for $pp \to g_1^{\mathrm{KK}} g_1^{\mathrm{KK}} / Q_1^{\mathrm{KK}} Q_1^{\mathrm{KK}} / g_1^{\mathrm{KK}} Q_1^{\mathrm{KK}} \to 2$ jets $+ 2G^{\mathrm{KK}}$ [19]: the topology of these processes from fat brane scenarios, consists of two back-to-back energetic jets and large missing transverse energy from the undetected gravitons (> 775 GeV). To improve the signal to background ratio a veto on isolated leptons is applied. The irreducible SM backgrounds are $Z(\to \ \nu\nu)jj$ and $W(\to l\nu)jj$. The signal and background were generated with PYTHIA [20], which does not generate the two jets from matrix element calculations but with initial and final state QCD radiation and parton showering. Therefore the results contain a systematic error due to this approximation. The generated events were further processed by the fast simulation and reconstruction programs of the ATLAS detector. The cascade decays were suppressed. On the other hand, the second KK level is suppressed by kinematics and the proton top flavor content ignored. The 5σ discovery reach in ATLAS for 100 fb^{-1} is shown in Fig. 4 (right).

3. Extra gauge bosons (Z', W')

CMS results for $pp \to Z' \to \mu\mu$ [7, 21]: the selection cuts to discriminate the signal from the background look for two opposite sign muons. The energy associated to the muon candidates is corrected for electromagnetic processes. The irreducible background is $Z \to \mu\mu$. Other backgrounds are ZZ, WZ, WW, $t\bar{t}$ at the level of few % of the Drell–Yan and further suppressed with selection cuts. Other potential backgrounds like cosmic, jet–jet, W–jet, $b\bar{b}$, hadron punch through and poorly measured $Z \to \mu\mu$, have not been studied yet. Authors claim that they will be also negligible compared to Drell–Yan. The signal and backgrounds were generated including the full $\gamma * /Z/Z'$ interference. Exotics decays are closed. The generated events were further processed by the full simulation and reconstruction programs of CMS including low (5 events) and high (25 events) luminosity pile-up. The studied systematic uncertainties include theoretical and muon and tracker misalignment uncertainties. Fig. 5 (left) shows the integrated luminosity needed to discover with a 5σ significance several Z' masses from different Extra Gauge Bosons models. The significance calculation was done with the likelihood-ratio-based test statistics (unbinned) given by:

$$\mathcal{S}_{\mathcal{L}} = \sqrt{2\ln(\mathcal{L}_{S+B}/\mathcal{L}_B)} > 5\,, \tag{3.1}$$

where $\mathcal{L}_{S+B}$ and $\mathcal{L}_B$ are the maximum likelihood value obtained in the full $S+B$ and B unbinned maximum likelihood fit, respectively. Without taking into account systematic uncertainties, an integrated luminosity < 0.1 fb^{-1}

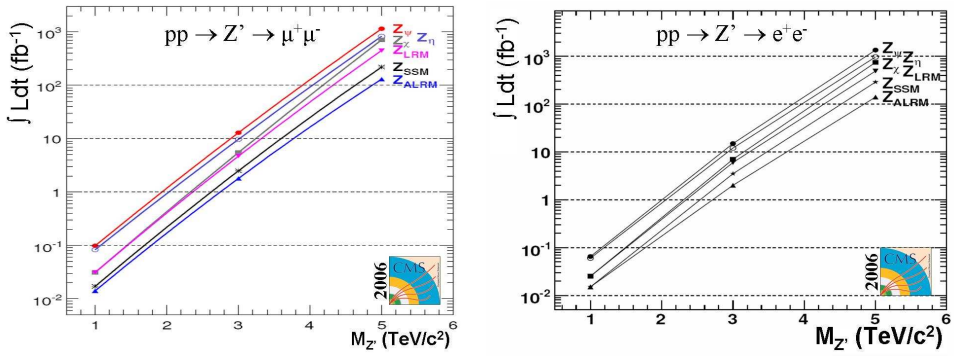


Fig. 5. Integrated luminosity needed to discover with a 5σ significance several Z' masses (in the two muons [7, 21] and two electrons [7, 10] channels respectively) for different heavy bosons theories in GUT; ZSSM is the Sequential Standard Model; ZLRM and ZALRM arise in the framework of Left–Right and Alternative Left–Right models. Symbols indicate fully-simulated-reconstructed mass-luminosity points, while lines are interpolations.

and non optimal alignment of the tracker and muon detectors, is enough to discover a Z' of 1 TeV ($\sim 50\%$ less data is needed to reach the same signal significance if the optimal alignment is achieved). Ten fb^{-1} is sufficient to reach 5σ significance at ~ 3 TeV for most (but not all) the Z' models considered if the optimal alignment is achieved. Finally, 100 fb^{-1} does not allow to obtain 5σ significance at ~ 5 TeV with only the $Z \to \mu\mu$ channel for any of the models considered. The mass reach is between 3.9 TeV and 4.9 TeV.

CMS results for $pp \to Z' \to ee$ [7, 10]: this analysis is the same as the one described in Sec. 2.4 (CMS results for $pp \to Z_1^{\mathrm{KK}}/\gamma_1^{\mathrm{KK}} \to ee$). Fig. 5 (right) shows the integrated luminosity needed to discover with a 5σ significance several Z' masses from different Extra Gauge Bosons models. The significance is calculated according to Eq. (2.2).

CMS results for $pp \to W' \to \mu\nu$ [7, 22]: the topology of this process consists of an isolated and well identified muon with high p_{T}. The analysis was done at low luminosity with ~ 3 pile up events, using full simulation and reconstruction. CMS looks for charged spin-1 W' from the Reference Model by Altarelli [23]. The irreducible background is $W \to \mu\nu$. Other backgrounds also studied are $Z \to \mu\mu$, WW, ZW and $t\bar{t}$. Such a boson is expected to be discovered, if exists, with a mass up to 4.6 TeV for an integrated luminosity of 10 fb^{-1}. The range can be expanded to 6.1 TeV for 300 fb^{-1} as shown in Fig. 6 (left). If no signs for a new W' boson appears, 95% C.L. exclusion limits of 4.7 TeV and 6.2 TeV can be set, respectively.

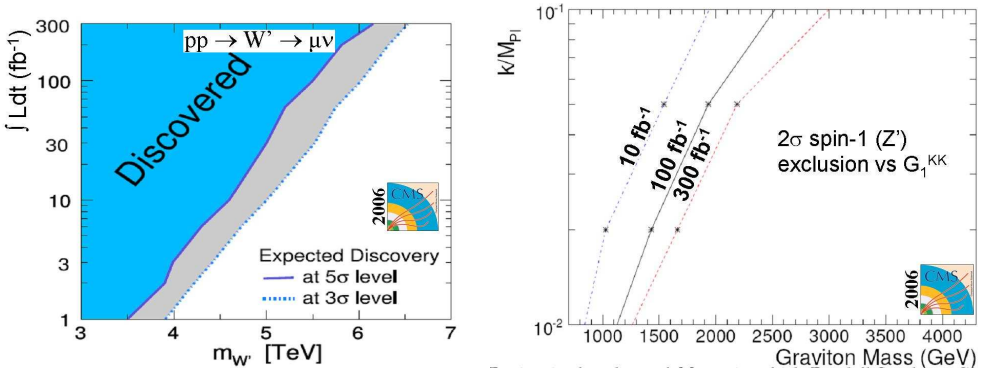


Fig. 6. Left: Integrated luminosity needed to discover with a 5σ significance several W' masses within the Reference Model by Altarelli [7, 22]. Right: Region in the plane $(c = k/M_{\mathrm{Pl}}, m(G_1^{\mathrm{KK}}))$ where RS G_1^{KK} can be distinguished from Z' with 2σ significance if one treats the two spin hypothesis symmetrically. The region which can be probed lies to the left of the lines [7].

4. How to discriminate between models

Once a resonance is discovered in the detector, the study of the angular distributions and the Forward–Backward asymmetry (A_{FB}) provides a way to investigate the nature of the new particles as it will be described in the following. In this section only the CMS discrimination method [7] is presented, but in Ref. [15] a complete description of the ATLAS discrimination method can be found.

In order to distinguish the spins of a spin-1 Z' boson and a spin-2 gravitons in a dilepton decay mode, CMS considers a unbinned likelihood ratio statistics incorporating the angles of the decay products as described in [24]. The statistical interpretation of this statistics is discussed in detail in [25], which also considers the possibility of spin 0. The method has been applied to fully-reconstructed Z' and RS gravitons. Details of the simulation, trigger and reconstruction are given in [7]. Fig. 6 (right) shows the region in the plane ($c = k/M_{\mathrm{Pl}}$, RS graviton mass) in which RS gravitons can be distinguished from Z' with 2σ significance if one treats two spin hypothesis symmetrically for a few representative values of the integrated luminosity. The results shown in the figure correspond to the long term misalignment scenario and the Z' production cross section is assumed to be equal to that of the RS graviton with the given c value. Since the production cross section falls rather steeply with mass, the integrated luminosity needed for spin discrimination increases with mass. For RS gravitons the production cross section scales with c^2, therefore, the integrated luminosity required for spin discrimination quickly increases as c gets smaller, and so does the number of signal events, because the larger background contamination. As discussed in [25], discriminating either spin-1 or spin-2 from spin-0 requires significantly more events than discriminating spin-2 from spin-1.

5. Conclusions

This conference report compiles the most recent results, from the experimental (simulation) point of view, on Extra Dimensions and Extra Gauge Bosons theories. In particular, the CMS and the ATLAS Collaborations analyses have been considered here. Almost all the analyses have included theoretical and experimental systematic errors in the discussion of the final results. The center of mass energy considered has been 14 TeV with low and/or high luminosity scenarios. In general, the first year of data taking at high luminosity will allow discovering BSM signatures up to few TeV with a 5σ significance. The conference report also addresses an extremely important subject: once a signature is discovered in the detector, what is the theoretical model that better fits the experimental data. It has been demonstrated that through the study of the angular distributions, the nature of the new particles can be disentangled.

REFERENCES

[1] N. Arkani-Hamed, S. Dimopoulos, G.R. Dvali, *Phys. Rev.* **D59**, 086004 (1999).

[2] L. Randall, R. Sundrum, *Phys. Rev. Lett.* **83**, 3370, 4690 (1999).

[3] K. Dienes, E. Dudas, T. Gherghetta, *Nucl. Phys.* **B537**, 47 (1999); I. Antoniadis, K. Benakli, M. Quiros, *Phys. Lett.* **B460**, 176 (1999).

[4] T. Appelquist, H.C. Cheng, B.A. Dobrescu, *Phys. Rev.* **D64**, 035002 (2001); G. Servant, T. Tait, *Nucl. Phys.* **B650**, 391 (2003).

[5] L. Vacavant, I. Hinchliffe, *J. Phys. G* **27**, 1839 (2001).

[6] J. Weng, C. Saout, G. Quast, A. De Roeck, M. Spiropulu, CMS NOTE 2006/129 (2006).

[7] CMS Collaboration, CERN/LHCC 2006-021, CMS TDR 8.2 26 Jun 2006.

[8] R. Cousins, J. Mumford, V. Valuev, CMS NOTE 2005/002.

[9] I. Belotelov *et al.*, CMS NOTE 2006/076 (2006).

[10] R. Clerbaux, T. Mahmoud, C. Collard, P. Mine, CMS NOTE 2006/083 (2006).

[11] I. Belotelov *et al.*, CMS NOTE 2006/104 (2006).

[12] M.C. Lemaire, V. Litvin, H. Newman, CMS NOTE 2006/051 (2006).

[13] H. Davoudiasl, J.L. Hewett, T.G. Rizzo, *Phys. Rev.* **D63**, 075004 (2001).

[14] V. Bartsch, G. Quast, CMS NOTE 2005/004 (2006).

[15] G. Azuelos, G. Polesello, *Eur. Phys. J.* **C39**, no. Suppl. 2, 1 (2005).

[16] G. Polesello, M. Prata, *Eur. Phys. J.* **C32**, s55 (2004).

[17] L. March, E. Ros, B. Salvachua, ATL-PHYS-PUB-2006-002 (2006).

[18] M. Kazana, *Acta Phys. Pol.* **38**, 447 (2007), these proceedings.

[19] P.H. Beauchemin, G. Azuelos, ATL-PHYS-PUB-2005-003.

[20] T. Sjostrand, S. Mrenna, P. Skands, *J. High Energy Phys.* **05**, 026 (2006).

[21] R. Cousins, J. Mumford, V. Valuev, CMS NOTE 2006/062 (2006).

[22] C. Hof, T. Hebbeker, K. Höpfner, CMS NOTE 2006/117 (2006).

[23] G. Altarelli, B. Mele, M. Ruiz-Altaba, *Z. Phys.* **C45**, 109 (1989).

[24] B.C. Allanach, K. Odagiri, M.A. Parker, B.R. Webber, *J. High Energy Phys.* **09**, 019 (2000).

[25] R. Cousins, *J. High Energy Phys.* **11**, 046 (2005); doi:10.1088/1126-6708/2005/11/046.